Macromolecules **1992,** *25,* 4605–4611

Dielectric Relaxation in Polymers by Molecular Dynamics Simulation

A. R. Tiller[†]

ICI Wilton Materials Research Centre, P.O. Box 90, Wilton, Middlesbrough, Cleveland, TS5 6QD, U.K.

Received November 27, 1991; Revised Manuscript Received April 7, 1992

ABSTRACT: A computational scheme for identifying and characterizing relaxations of polymers which are important in their dielectric behavior over a frequency range from about 10^9 to 10^{13} Hz is developed. The method utilizes molecular dynamics simulations and involves calculation of the dipole autocorrelation function for identifying the frequencies of the characteristic motions which are important in dielectric relaxation. Analysis of polystyrene reveals localized motions of segments of the polymer chain, including crankshaft type motions of the backbone and librational motions of the pendant phenyl rings. The polyimide Kapton is also investigated, and interesting nonlocal motions involving many repeat units of the chain are found. The low-frequency Kapton motions are rather like those of a piece of string which is twisted at one end. Despite the simplicity of the method, it can be used to find out what types of motion take place during dielectric relaxation and hence aids fundamental understanding of dielectric dispersion in polymers.

1. Introduction

An understanding of molecular level influences on dielectric properties of polymers is fundamental to the development of materials for use in many types of application. In particular, the behavior of polymer chains under the influence of microwave-frequency radiation is relevant for microwave oven components, packaging of microwave foods, electronics and communication uses, and even stealth radar absorption. The microwave-frequency region can be considered to lie approximately in the range 10^8–10^{11} Hz, although higher frequencies are also of interest.[1]

A material for use in microwave oven components should ideally have a high relative permittivity and a low dielectric loss in the microwave region, a combination of which leads to a high reflection coefficient. Stealth materials, on the other hand, should have high absorption coefficients and therefore low permittivity and high loss. With some exceptions,[2] pure polymers tend to exhibit low permittivities and low losses and are suited for electronics and communication uses. Optimization of the relative permittivity and dielectric loss, as well as various other physical properties of the polymer, is important for these purposes.

There are many mechanisms by which polarization can occur in polymers.[3,4] One important mechanism in microwave-frequency electric fields is dielectric relaxation, in which the permanent dipoles of the polymer chain try to align favorably with the field direction through conformational changes. This type of relaxation is most effective when the frequency of the applied electric field oscillation and that of a characteristic, or natural, motion of the polymer chain come into resonance, especially when the characteristic motion is associated with a large change in the dipole moment vector. Large-scale characteristic motions such as those involved in the glass transition are generally too slow to contribute to microwave dielectric relaxation unless the temperature is well above T_g, and it is local motions involving small segments of the chain which are generally the most important.[1]

The dielectric relaxation spectra of polymers consist of broad bands. Atactic polystyrene, for example, shows a broad maximum in the dielectric loss tangent ($\tan \delta = \epsilon''/\epsilon'$) between 10^{11} and 10^{13} Hz.[5] Even a relaxation arising from a single type of conformational motion gives rise to a broad band because its frequency will vary from one region to another depending upon the local environment. The purpose of this work is to find the nature of characteristic motions which contribute to the dielectric relaxation within a given band in the observed spectrum.

The method described in this work uses molecular dynamics (MD) simulations. Characteristic molecular motions which give rise to large changes in the dipole moment vector are distinguished from other characteristic motions by making use of the dipole autocorrelation function (DACF). These characteristic motions can then be analyzed using a Fourier transform filtering technique, which enables the motions of interest to be visualized on a graphics workstation.

2. Identifying Characteristic Motions in Polymers

The usual method of identifying characteristic motions of molecules is normal-coordinate analysis (NCA).[6,7] This method has been used successfully in calculating phonon dispersion curves and frequency distributions in polymers,[8] and low-frequency motions such as the longitudinal acoustic modes in crystalline polyethylene have also been studied.[9] However, NCA has limitations which make it necessary to find alternative methods for studying the characteristic motions occurring in dielectric relaxation. Perhaps the most important is that it assumes small-amplitude vibrations about a fixed equilibrium geometry, so that motions which pass from one low-energy chain conformation to another cannot be investigated. This type of motion is likely to be of great importance in dielectric relaxation. Another drawback with NCA is the assumption that all vibrations are harmonic. This is not necessarily appropriate for the low-frequency motions of polymer chains.

An alternative method of identifying characteristic motions using molecular dynamics has recently been demonstrated for proteins by Osguthorpe and co-workers.[10] The MD method not only avoids the major drawbacks of NCA but also has the potential for investigating the influence of interactions between neighboring chains in the bulk material.

[†] Current address: Biosym Technologies Ltd., Unit 17, INTEC 2, Wade Road, Basingstoke, RG24 0NE, U.K.

0024-9297/92/2225-4605$03.00/0

The MD-based approach involves analysis of the "coordinate trajectories", which are the time-dependent Cartesian coordinates of each atom in the molecule. The coordinate trajectories are generally stored as a series of data blocks, each one containing the Cartesian coordinates of the atoms at a given instant of time during the MD simulation.

If coordinate trajectories are Fourier transformed to the frequency domain, characteristic motions can be identified from the frequency distribution function which is readily obtained. A filtering function can then be applied before the frequency domain coordinate trajectories are inverse Fourier transformed back into the time domain. This allows characteristic motions of interest to be isolated and visualized by animating the filtered time-domain trajectories on a graphics workstation. For example, by this mean a 10-ps MD simulation can be used to reveal motions with time periods up to around 10^{-11} s, or frequencies as low as 10^{11} Hz (3 cm^{-1}).

3. The Dipole Autocorrelation Function

Not all characteristic motions of a polymer chain are important in the dielectric relaxation process. For this reason, the following method was devised in order to obtain the frequencies of the important motions. The method uses the dipole autocorrelation function (DACF)[11] of the polymer chain and allows the natural frequencies for motions with significant dipole moment oscillations to be identified.

During the MD simulation the dipole moment vector of the polymer chain is calculated and saved every femptosecond. The saved dipole moment vectors are then used to calculate the DACF, $C(t)$, given by

$$C(t) = \frac{\langle \mathbf{M}(t)\cdot\mathbf{M}(0)\rangle}{\langle \mathbf{M}(0)\cdot\mathbf{M}(0)\rangle}$$

where $\mathbf{M}(t)$ is the dipole moment vector of the molecule after a time t. The angled brackets denote an ensemble average over many conformations at the same *elapsed* time. Here this average is obtained by a standard method in MD of allowing many points along a single trajectory to be the starting point for a new elapsed time.[12]

Physically, the DACF gives a measure of the memory which the molecule retains at time t for its original dipole moment vector at the time origin, $t = 0$. For a molecule undergoing random thermal motions, it follows that $C(0) = 1$ and that $C(t) \rightarrow 0$ as $t \rightarrow \infty$. In between these two extremes, the DACF can show a complicated time variation. Oscillations may be observed at frequencies corresponding to natural motions which exhibit significant dipole moment variation—the very motions we wish to identify. A frequency spectrum for these motions is obtained by Fourier transformation of the DACF.

4. Practical Considerations

(i) Resolution of the DACF Frequency Spectrum. The frequency resolution, R, of the spectrum depends upon the length of time, T_D, for which the DACF has been calculated. Due to the nature of the averaging technique used, T_D is somewhat less than the total MD simulation time. If T_D is measured in femptoseconds, R is given in wavenumbers by

$$R = 33356.46/T_D$$

For example, if the DACF is known from $t = 0$ to 10 ps, the frequency resolution is about 3.3 cm^{-1}.

(ii) Frequency Resolution and Animation of the MD Trajectories. Visualization of a characteristic motion identified by the MD/DACF method is achieved by the method of Fourier transforming the coordinate trajectories into frequency space, applying a filter window containing the natural frequency of the motion, inverse Fourier transforming back to the time domain, and then animating the filtered motion on a graphics workstation. This animation consists of a series of snapshots (frames) which are displayed in sequence. Each frame shows the conformation of the molecule at a given instant during the simulation. For clear visualization and analysis, the animation must consist of perhaps 20 frames for each time period of the characteristic motion.

Fourier transformation of the coordinate trajectories to frequency space is achieved with a resolution which is determined by the length of the MD simulation. The resolution must typically be less than 10 cm^{-1} or so in order that the filtering function can be applied, calling for simulation times of at least 3.5 ps. The two requirements of long enough simulation times and of storing around 20 frames per time period make the method impractical for visualizing motions with very short time periods (high frequencies). Nor can motions with very long time periods be observed, as it is not possible to carry out MD simulations covering at least a sizable portion of that time period. The practical limits for convenient analysis of characteristic motions using current computer technology are roughly 10^9–10^{13} Hz.

(iii) Accuracy. Just as the accuracy of a normal-coordinate analysis depends upon the force constants assumed, the accuracy of the MD/DACF method in predicting the frequencies of characteristic motions depends upon the molecular dynamics force field.[13] The consistent valence force field[14] used in this work was originally created for modeling proteins and peptides and has been extended to handle more general systems with similar functional groups. Torsional motions have the greatest influence upon the conformation of polymer chains,[15] and so it is important that the force field models these accurately.

While it is desirable to use as accurate a force field as possible, small inaccuracies will not necessarily invalidate the use of the method for its original purpose. This purpose is not to predict accurately the frequencies of characteristic motions of a polymer chain in a given local environment but rather to identify and characterize motions which contribute to the experimentally observed dielectric relaxation in a broad frequency band.

The results obtained from the MD/DACF method will also depend upon the accuracy of the calculation of the dipole moment vector, which in turn depends upon the assignment of partial charges to each atom in the polymer chain before the MD simulation is carried out. This effect is not critical because it is the *change* in the permanent dipole moment vector with conformation of the polymer chain which is important in the methodology and not the accuracy of the calculated dipole moment vector itself. In this work, a bond incremental method of charge assignment was used.[16]

5. Results

Results are presented here for polystyrene and Kapton, which have the structures

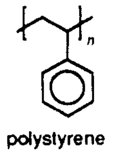

polystyrene

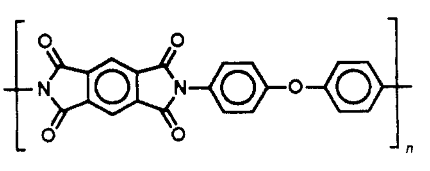

Kapton

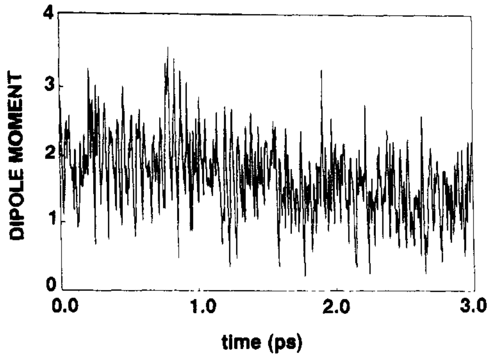

Figure 1. Magnitude of the dipole moment for a single, isolated chain of isotactic polystyrene during 3.0 ps of a molecular dynamics simulation.

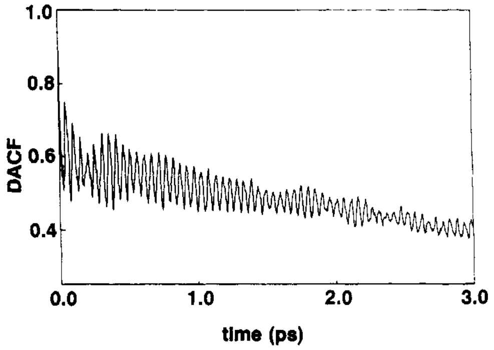

Figure 2. Dipole autocorrelation function for a single, isolated chain of isotactic polystyrene obtained from molecular dynamics simulation.

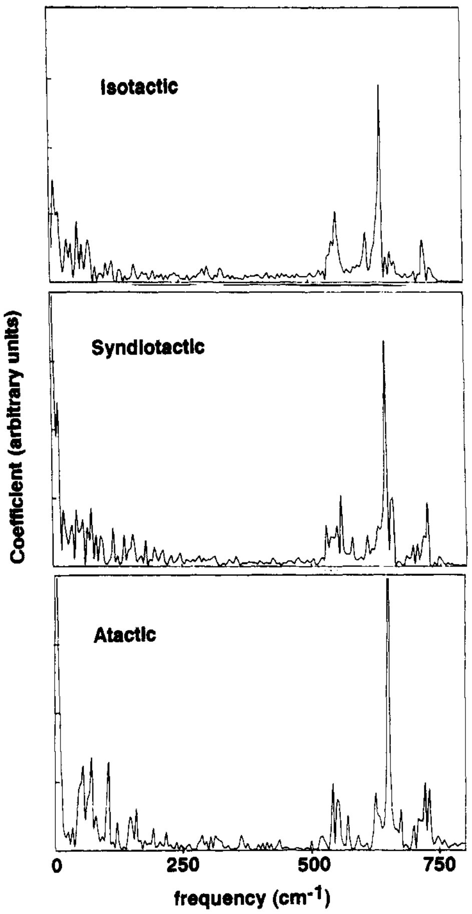

Figure 3. Fourier transforms of the calculated dipole autocorrelation functions for single chains of isotactic, syndiotactic, and atactic polystyrene.

(i) Polystyrene. Single chains of isotactic, syndiotactic, and atactic polystyrene consisting of 25 repeat units were constructed and relaxed using molecular mechanics[17] with the DISCOVER program[14] to obtain low-energy conformations. This geometry optimization prevents the formation of local "hot spots" in the MD simulations. For each chain, initialization of the dynamics was carried out to ensure full equilibration at the simulation temperature of 300 K, after which the simulation was continued for a further 10 ps with a time step of 0.5 fs.

Dipole moment vectors for the isolated chain were calculated from the formula

$$\mathbf{M}(t) = \sum_{i=1}^{N} e_i \mathbf{r}_i$$

(where e_i is the partial charge and $\mathbf{r}_i(t)$ the position vector for atom i). $\mathbf{M}(t)$ was calculated and saved every femptosecond during the simulation.

Figure 1 shows a plot of $|\mathbf{M}(t)|$ for the first 3 ps of a MD simulation of isotactic polystyrene. While it is difficult to see any regularity in this plot, the corresponding DACF given in Figure 2 clearly shows regular oscillations at a frequency of around 2×10^{13} Hz (650 cm^{-1}).

Figure 3 shows Fourier transformed DACFs obtained from MD simulations on single, isolated chains of isotactic, syndiotactic, and atactic polystyrene. These are typical examples obtained from a number of different simulations rather than strict averages. In each plot, the motions at around 650 cm^{-1} are clearly visible. There are also a number of important motions occurring at frequencies below about 120 cm^{-1}, and these motions will contribute to the dielectric relaxation in the frequency range 10^{11}–10^{13} Hz with which we are most concerned.

The resolution of the plots in Figure 3 is about 4.2 cm^{-1}. Longer simulations would enable higher resolution which would split many of the peaks in the spectrum, but it is most likely that peaks occurring less than 4 cm^{-1} apart are due to the same types of motions occurring in different local environments. We aim only to identify the general motion types which contribute to the broad experimental spectrum.

For reasons which will become apparent, the positions of low-frequency peaks in the spectra of Figure 3 vary to a small extent with the starting geometry used in the MD simulation. However, the positions of the higher frequency peaks (above 500 cm^{-1}) are much less dependent upon starting conformation. Differences between the isotactic, syndiotactic, and atactic polystyrene chains can be observed in the higher frequency region, reflecting the different types of local environments generated by the different tacticities.

The low-frequency motions in Figure 3 were visualized using the Fourier transform filtering technique. Each plot in Figure 3 shows a large contribution from motions below 20 cm^{-1}, and animation of the filtered trajectories shows that these involve rotation about backbone C–C bonds, similar in nature to the crankshaft motions proposed by Boyer[18] and Schatzki[19] and investigated by Boyd and Breitling.[20]

Motions in the range 35–100 cm^{-1} consist mainly of librational motions of the phenyl groups about the bond which connects the ring to the polymer backbone. Figure 4 shows two segments of the isotactic polystyrene chain taken from a snapshot of the simulation. In segment A, the phenyl groups on adjacent repeat units are fairly well separated due to the conformation of the chain backbone. However, in segment B the phenyl rings on adjacent repeat units interact more strongly.

The librational frequencies of the phenyl rings depend upon the local environment. For example, the motions between 35 and 45 cm^{-1} consist of librations of phenyl groups which are relatively unhindered, such as those at the chain ends. Between 48 and 58 cm^{-1} it is possible to

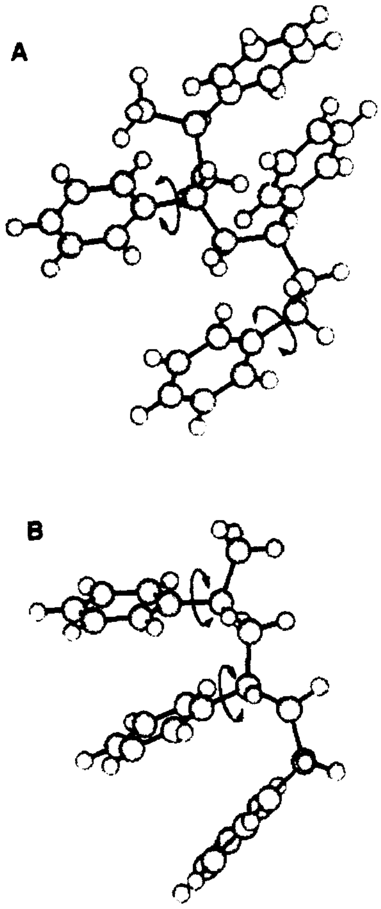

Figure 4. Typical segments taken from an isolated chain of isotactic polystyrene during the molecular dynamics simulation. A and B show different local environments for librational motions of phenyl rings.

observe in-phase librational motions of two adjacent phenyl groups such as those in segment A of Figure 4. Around 80 cm^{-1}, in-phase librations of more crowded adjacent phenyl groups can be found, as well as some near out-of-phase librations. As is intuitively expected, the out-of-phase librational motions occur at higher frequencies than the corresponding in-phase motions. Figure 5 shows variations in the dihedral angles of selected bonds connecting phenyl rings to the chain backbone. In-phase and near out-of-phase librational motions of adjacent phenyl groups can clearly be seen in parts b and c of Figure 5, respectively.

It is clear that the important relaxations in polystyrene chains at frequencies below 120 cm^{-1} involve torsional motions. This is in accord with the calculations of Snyder et al.,[21] whose analysis of single, disordered polymethylene-like chains revealed that torsional motions dominate the molecular dynamics at frequencies below 140 cm^{-1}.

The librational motions of the phenyl rings are not completely localized; they are coupled to each other and also to the backbone torsional motions which occur at frequencies below 20 cm^{-1}. Thus the librational motions influence the backbone conformation of the chain, and this coupling to the "chain shape" explains the dependence of the low-frequency peak positions in Figure 3 upon the starting conformation used in the MD simulation. This observation is in contrast with evidence from the MD simulations of Buchner and Dorfmuller on short styrene chains in the bulk that side-group librations are not strongly coupled to other degrees of freedom.[22] Buchner and Dorfmuller also find that backbone torsions dominate the chain motions between about 20 and 80 cm^{-1} and that phenyl ring librations occur mainly at higher frequencies. Differences compared to the results presented here might be attributed to the form of the force field which was used and to the difference between bulk and isolated chain simulations. It is interesting that Buchner and Dorfmuller's results place the torsional and librational motions closer to the center of the experimentally observed dielectric relaxation spectrum.

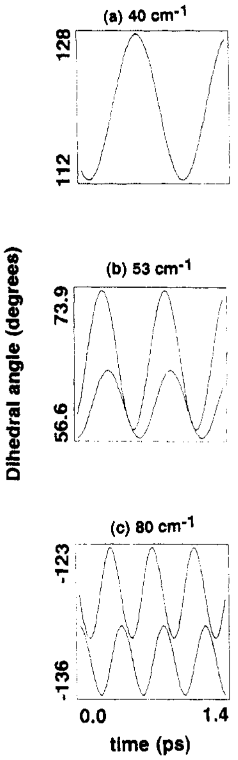

Figure 5. Plots showing the time variation of the dihedral angle about the bond joining phenyl rings to the polystyrene backbone for rings in different local environments: (a) relatively unhindered ring at a chain end, (b) two adjacent rings librating in-phase, (c) near out-of-phase librational motion of adjacent phenyl rings. The characteristic frequencies of these motions increase from (a) to (c).

Analysis of the higher frequency motions identified in Figure 3 shows them to consist of various highly localized vibrational modes of the phenyl rings. For example, the motion at around 647 cm^{-1} corresponds to the A_{2u} ring flexing mode which is observed experimentally at 670 cm^{-1} in benzene. These vibrational modes are not strongly coupled to the backbone torsional motions, which explains why the positions of the higher frequency peaks in the spectra of Figure 3 are not very dependent upon the starting conformation used in the MD simulation.

The frequencies of the phenyl ring vibrations appear to be too high to contribute to the experimentally observed dielectric relaxation between 10^{11} and 10^{13} Hz. It is possible that the assignment of partial atomic charges before the MD simulation gives an unrealistically large change in the dipole moment vector associated with these modes and that their contribution to dielectric relaxation is overestimated in this work.

The behavior of bulk polystyrene may not be accurately represented by MD simulations involving short segments of isolated polystyrene chains. However, the computational effort involved in simulating the bulk is much greater than for the isolated chain calculations, and there are also new problems associated with the application of appropriate boundary conditions and with the correct treatment of the long-range Coulombic interactions. Here, we present the results of a very simple simulation of an amorphous cell of bulk atactic polystyrene subject to periodic boundary conditions.

A representative amorphous cell was constructed from a single chain of 50 repeat units of polystyrene using an

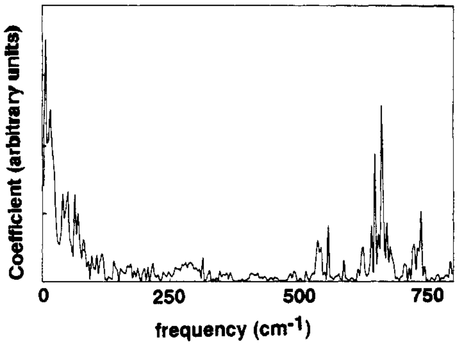

Figure 6. Fourier transform of the dipole autocorrelation function obtained from a MD simulation of bulk polystyrene.

adaptation of the method of Theodorou and Suter.[24] A MD simulation of this cell was then carried out for a time period of 5.0 ps after equilibration at 300 K, using a cutoff distance of 10.0 Å to determine the maximum distance over which atom pair interactions are considered to be nonzero. Long-range Coulombic interactions are still significant at distances greater than this cutoff, but in this initial work no corrections were attempted. Corrections using, for example, the Ewald summation technique[23] could readily be made.

Figure 6 shows the Fourier transformed DACF calculated from the dipole moment vectors saved during the bulk simulation of atactic polystyrene. Comparison with Figure 3 shows the main features of the single-chain result are preserved in the bulk simulation. The relative intensities of higher and lower frequency peaks for the bulk simulation hint at an increased contribution from the low-frequency motions compared to the isolated chain case. However, more thorough work is required to prove whether or not this is a real effect caused by the presence of the surrounding molecules.

Because of the shorter simulation time, the frequency resolution in Figure 6 is only half as good as that in Figure 3. However, when comparing like with like, the bulk simulation shows a larger number of peaks in its DACF spectrum than the single-chain simulation. This is a consequence of the greater variety of local environments in the bulk and therefore the greater range of frequencies over which a single type of local motion can occur.

(ii) Kapton. Kapton is the trade name of a polyimide made by Du Pont and marketed commercially as a film with a major use in flexible electronic circuitry. Molecular dynamics simulations were carried out on four segments of single, isolated Kapton chains. Two different lengths, the first consisting of 197 atoms and the second of 392 atoms, were used for each of the two different starting conformations, helical and zigzag.

Figure 7 shows the DACF frequency spectra obtained from the MD simulations for the two helical chains. The major contributions at low frequencies are from two types of motion, one occurring at frequencies below 20 cm^{-1} and the other occurring at around 110 cm^{-1}. Analysis of the motion at 110 cm^{-1} shows a complex local motion of single repeat units of the Kapton chain, involving near out-of-phase torsional motions about the nitrogen–phenyl bonds.

The motions below 20 cm^{-1} are of particular interest because the frequency of the spectral peak can be seen to depend upon the length of the Kapton chain segment used in the simulation (see Figure 7). This suggests that the motion involves the whole chain segment and is not localized in one small region. Visualization and analysis of the motion using the Fourier transform filtering method indicate that this is indeed the case. Figure 8 shows two superimposed snapshots taken from the filtered animation illustrating the extremes of the motion observed in the 197 atom segment. Also shown are graphs of (a) end-to-end distance, (b) the length of a single repeat unit, and (c) the dihedral angle about one bond of the –O– linkage. The animation shows that the major motion is rather like that of a piece of string which is twisted at one end, with the twist passing down the chain from one end to the other. This twisting is strongly coupled to a flexing motion of single repeat units. Also observed is a motion in which the average helical repeat distance expands and contracts in a springlike fashion.

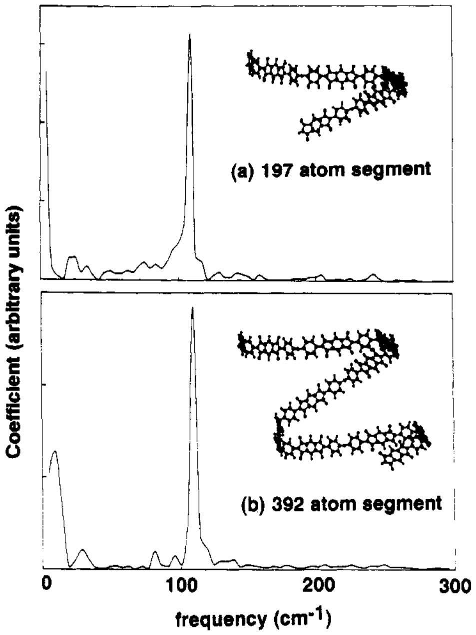

Figure 7. Fourier transform of the DACF for single isolated chains of Kapton in a helical geometry: (a) 197 atom segment and (b) 392 atom segment.

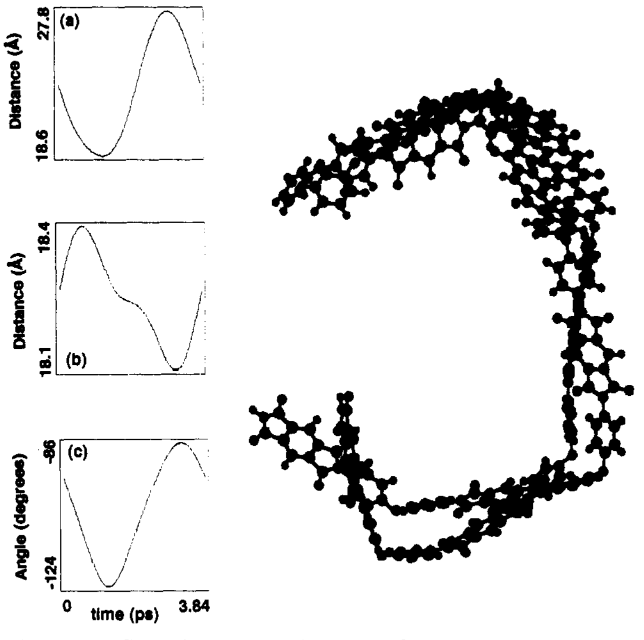

Figure 8. Snapshots from the filtered motion of a 197 atom segment of Kapton. The two extremes of the chain vibrational mode occurring below 10 cm^{-1} are illustrated, along with graphs showing the time variation of (a) end-to-end distance, (b) the length of one repeat unit, and (c) the dihedral angle about a bond in one of the –O– linkages.

Using molecular mechanics, we have estimated that the relaxed zigzag chain conformation does not differ greatly in energy from the relaxed helical conformation. Figure 9 shows the DACF frequency spectra obtained for the zigzag chains, and it is interesting to compare these with the results in Figure 7. The peaks at around 110 cm^{-1} are

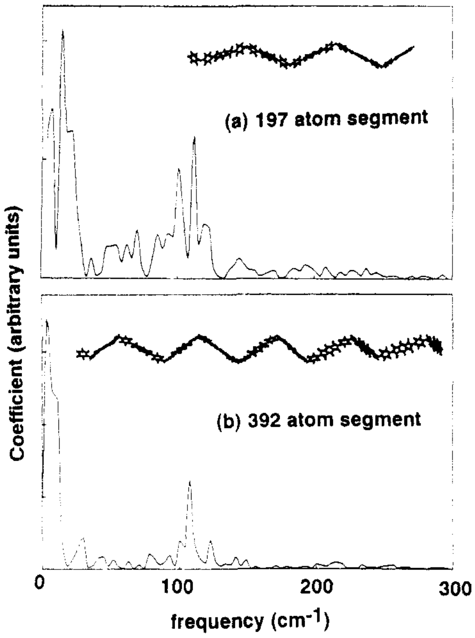

Figure 9. Fourier transform of the DACF for single isolated chains of Kapton in a zigzag geometry: (a) 197 atom segment and (b) 392 atom segment.

still evident, but the lower frequency peaks are more pronounced and different in shape. Animation again shows that the major motion is like twisting a piece of string, but this time the repeat unit flexing is not so evident. This can be rationalized with the string analogy; twisting a curled up piece of string causes the string to flex and change its shape a lot more than twisting a relatively straight piece of string.

For the helical conformation, increasing the chain length from 197 to 392 atoms appears to increase the frequency of motions under 20 cm^{-1}. In contrast, the zigzag chain shows the opposite effect. A possible explanation may be that the helical segment exhibits a springlike motion, whereas the zigzag segment exhibits a wavelike motion. If the helical coil is likened to a spring, then the nonbonded interactions between the loops of the chain will affect the forces exerted when the spring expands and compresses. It is reasonable to expect the longer, more coiled, chain to have a higher "force constant" and therefore to have a higher frequency springlike motion. Wavelike motions show the opposite behavior, moving to lower frequencies as the chain length is increased.

6. Discussion

Several types of molecular theory have been developed to account for dielectric relaxation in polymers.[1,4] These include barrier models,[20,25-29] which consider the rate of motions across a potential energy barrier from one low-energy conformation to another, and local mode theories,[30,31] which treat the polymer chain motions as a superposition of normal modes. The so-called γ and δ dispersions[1] are characterized by short relaxation times, and depending upon the temperature, they are potentially active at microwave frequencies. Molecular mechanisms proposed for the γ and δ relaxations which have been investigated using the above models include rotation of a polar group in a side chain, damped oscillations of a local vibrational model of a dipolar group, and crankshaft motions.[18-20]

Recent advances in computing technology have given molecular dynamics simulations the potential to greatly improve our understanding of the molecular mechanisms of dielectric relaxation in polymers. A MD simulation contains information about many different types of motion and about the interaction between different motions. Furthermore, the motions can be selectively viewed using the Fourier transform filtering technique. Combined with methods for determining which of the observed motions give a significant contribution to dielectric relaxation, the method provides a fundamental understanding which cannot be obtained from the earlier molecular theories. Although the motions which can usefully be studied by MD simulations are at present restricted to the approximate frequency range 10^9–10^{13} Hz, this situation will improve as computer speed and memory increase, especially with the optimization of MD programs for massively parallel computers.

Use of the dipole autocorrelation function in the theory of dielectrics is long established,[32] as is its application to molecular theories of dielectric relaxation in polymers.[11] The usefulness of molecular dynamics in the study of dielectric behavior has also been exploited; for example, the dielectric properties of liquid water have been investigated through calculation of dipole autocorrelation functions obtained from big MD simulations.[33]

The relationship between molecular behavior and dielectric phenomena is very complex,[34] and computational methods of predicting dielectric properties must take account of long-range Coulombic interactions and the influence of the particular boundary conditions applied in the simulation.[35,36] However, the simple methodology presented here does give substantial insight into the nature of molecular level processes which influence the dielectric relaxation of polymers.

Acknowledgment. I am grateful to Dr. John Kendrick for some stimulating discussions and to Dr. David Rigby for constructing the amorphous cells of polystyrene which were used in the bulk MD simulation.

References and Notes

(1) Bur, A. J. *Polymer* **1985**, *26*, 963.
(2) Pohl, H. A.; Engelhardt, E. H. *J. Phys. Chem.* **1962**, *66*, 2085. Pohl, H. A.; Pollak, M. *J. Chem. Phys.* **1977**, *77*, 4031. Pohl, H. A. *J. Polym. Sci., Part A* **1986**, *24*, 3057.
(3) Hedvig, P. *Dielectric Spectroscopy of Polymers*; Hilger: Bristol, U.K., 1977.
(4) McCrum, N. G.; Read, B. E.; Williams, G. *Anelastic and Dielectric Effects in Polymeric Solids*; Wiley: New York, 1967.
(5) Amrhein, E. M. *Kolloid Z. Z. Polym.* **1967**, *38*, 216.
(6) Wilson, E. B.; Decius, J. C.; Cross, P. C. *Molecular Vibrations*; McGraw Hill: New York, 1955.
(7) Painter, P. C.; Coleman, M. M.; Koenig, J. L. *The Theory of Vibrational Spectroscopy and its Application To Polymeric Materials*; Wiley: New York, 1982.
(8) Piseri, L.; Zerbi, G. *J. Chem. Phys.* **1968**, *48*, 3561.
(9) Tasumi, M.; Shimanouchi, T. *J. Chem. Phys.* **1965**, *43*, 1245. Tasumi, M.; Krimm, S. *J. Chem. Phys.* **1967**, *46*, 755.
(10) Sessions, R. B.; Dauber-Osguthorpe, P.; Osguthorpe, D. J. *J. Mol. Biol.* **1988**, *209*, 617. Dauber-Osguthorpe, P.; Osguthorpe, D. J. *J. Am. Chem. Soc.* **1990**, *112*, 7921.
(11) Williams, G. *Chem. Rev.* **1972**, *72*, 55.
(12) Allen, M. P.; Tildesley, D. J. *Computer Simulation of Liquids*; Clarendon: Oxford, U.K., 1987.
(13) Ermer, O. *Struct. Bonding* **1976**, *27*, 161.
(14) DISCOVER Version 2.7, Biosym Technologies Inc., San Diego, CA.
(15) Flory, P. J. *Statistical Mechanics of Chain Molecules*; Hanser: Munich, 1989.
(16) The charge on an atom is given by $q_i = \sum_j \delta_{ij}$, where δ_{ij} is the bond increment between an atom of type i and one of type j. The sum is over all atoms bonded to atom i.
(17) Burkert, U.; Allinger, N. L. *Molecular Mechanics*; Caserio, M. C., Ed.; ACS Monograph Series 177; American Chemical Society: Washington, DC, 1982.
(18) Boyer, R. F. *Rubber Chem. Technol.* **1963**, *34*, 1303.
(19) Schatzki, T. F. *J. Polym. Sci.* **1962**, *57*, 496; *Polymer Prepr. (Am. Chem. Soc., Div. Polym. Chem.)* **1965**, *6*, 646; *J. Polym. Sci., Part C* **1966**, *14*, 139.
(20) Boyd, R. H.; Breitling, S. M. *Macromolecules* **1974**, *7*, 855.
(21) Snyder, R. G.; Strauss, H. L. *J. Chem. Phys.* **1987**, *87*, 3779.

(22) Buchner, M.; Dorfmuller, Th. In *Reactive and Flexible Molecules In Liquids*; Dorfmuller, Th., Ed.; Kluwer: Lancaster, U.K., 1989; pp 181–198.
(23) See, for example: Heyes, D. M. *J. Chem. Phys.* **1981**, *74*, 1924.
(24) Theodorou, D. N.; Suter, U. W. *Macromolecules* **1985**, *18*, 1467.
(25) Debye, P. *Polar Molecules*; Dover: New York, 1945.
(26) Frohlich, H. *Theory of Dielectrics*; Oxford, U.K., 1949.
(27) Hoffman, J. D. *J. Chem. Phys.* **1955**, *23*, 1331.
(28) Ishida, Y.; Yamafuji, K. *Kolloid Z.* **1961**, *177*, 97.
(29) Hoffman, J. D.; Williams, G.; Passaglia, E. *J. Polym. Sci., Part C* **1966**, *14*, 173.
(30) Yamafuji, K.; Ishida, Y. K. *Kolloid Z.* **1962**, *183*, 15.
(31) Saito, N.; et al. Molecular Motion in Solid State Polymers. *Solid State Phys.* **1963**, *14*, 343.
(32) Glarum, S. H. *J. Chem. Phys.* **1960**, *33*, 1371.
(33) Lie, G. C.; Clementi, E. *Phys. Rev. A* **1986**, *33*, 2679.
(34) Madden, P.; Kivelson, D. *Adv. Chem. Phys.* **1984**, *56*, 467.
(35) Kivelson, D.; Madden, P. *J. Phys. Chem.* **1984**, *88*, 6557.
(36) Neumann, M. *Mol. Phys.* **1983**, *50*, 841. Neumann, M.; Steinhauser, O.; Pawley, G. S. *Mol. Phys.* **1984**, *52*, 97.

Registry No. Kapton (SRU), 25036-53-7.